DALTON

Syntheses and molecular structures of ruthenium carbonyl complexes containing 1,2-naphthoquinone-1-oximate ligands

Kenneth Ka-Hong Lee and Wing-Tak Wong *

Department of Chemistry, The University of Hong Kong, Pokfulam Road, Hong Kong

The reaction of $[Ru_3(CO)_{12}]$ with 1-nitroso-2-naphthol (referred to as 1,2-naphthoquinone-1-oxime, Hnqo) in tetrahydrofuran (thf) at room temperature gave two isomeric mononuclear complexes, *trans*-$[Ru\{\eta^2\text{-}N(O)C_{10}H_6O\}_2(CO)_2]$ **1a** and *cis*-$[Ru\{\eta^2\text{-}N(O)C_{10}H_6O\}_2(CO)_2]$ **1b**. Compound **1b** could be converted to **1a** quantitatively in acidic media. Reaction of **1a** with acetylpyridine in the presence of trimethylamine *N*-oxide afforded *trans*-$[Ru\{\eta^2\text{-}N(O)C_{10}H_6O\}_2\{NC_5H_4C(O)CH_3\}(CO)]$ **2** in which one of the carbonyls was replaced by an acetylpyridine moiety. Similarly, complex **3**, *trans*-$[Ru\{\eta^2\text{-}N(O)C_{10}H_6O\}_2(NCMe)(CO)]$ was also obtained in high yield if acetonitrile was used instead of the acetylpyridine. When the reaction of $[Ru_3(CO)_{12}]$ and 1-nitroso-2-naphthol was carried out in refluxing thf for 1 h, two minor products $[Ru_3(\mu\text{-}\eta^3\text{-}ONC_{10}H_6O)_2(CO)_8]$ **4** and $[Ru_3\{\mu\text{-}\eta^2\text{-}N(H)C_{10}H_6O\}\{\mu\text{-}\eta^2\text{-}N(H)C_{10}H_4(O)NOC_{10}H_6\}(CO)_8]$ **5** were isolated in addition to **1a** and **1b**. Clusters **4** and **5** consisted of an open triruthenium metal core with the two nqo ligands (in **4**) and two quinone–imine type ligands (in **5**) bridging the open edge in a $\mu\text{-}\eta^3$ and a $\mu\text{-}\eta^2$-manner respectively.

The chemistry of transition-metal complexes containing nitrogen oxides has drawn considerable attention. The main stimuli for this investigation comes from the widespread occurrence of nitrogen oxides as environmental hazards produced in many combustion processes.[1] It is well documented that nitro and nitroso compounds can undergo deoxygenation to give products *via* the formation of imido intermediates. A general synthetic route for the formation of co-ordinated imido species, $[M_3(CO)_{10}(\mu_3\text{-}NR)]$ where (M = Fe, Ru or Os; R = Ph or tolyl) has been developed from the reactions between the transition-metal clusters, $[M_3(NCMe)_n(CO)_{12-n}]$ (n = 0–2) and nitro- or nitroso-arenes.[2] These imido clusters have also been proposed as intermediates in the catalytic reduction of nitrobenzene to aniline.[3] Recently, we have also demonstrated the formation of an unprecedented cluster, $[Ru(\mu_3\text{-}NPh)_2(\mu\text{-}\eta^2\text{-}ONPh)_2(CO)_7]$ in which both phenylimido and nitrosobenzene moieties are present.[4] In order to extend our investigations according to the above synthetic approach, nitroso compounds with *ortho*-substituted functionalities have been selected since there has been relatively little study on this class of compounds. 1-Nitroso-2-naphthol (referred to as 1,2-naphthoquinone-1-oxime) shows a different reactivity pattern compared to nitrosoarenes since it can undergo tautomerization to give an oxo–oxime[5] as shown in Scheme 1.

1-Nitroso-2-naphthol is currently used as a complexing agent in cobalt analysis[6] and is also used as a UV and thermal stabilizer.[7] However, co-ordination compounds containing this ligand are comparatively rare. Structural analyses of these complexes reveal a unique co-ordination mode in which the naphthoquinone–oxime moieties act as a bidentate ligand which chelate to the central metal atom through the nitroso N atom and the naphtholic O atom.[8] Alper and Edward[9] demonstrated the reductive deoxygenation of *p*-nitrosophenols by $[Fe(CO)_5]$ which afforded 4,4′-dihydroxyazobenzene. Charalambous *et al.*[10] further studied the reaction of $[Fe(CO)_5]$ towards 1,2-naphthoquinone-2-oxime and 5-methoxy-1,2-quinone-2-oxime (5-methoxy-2-nitrosophenol) which gave 2-amino-*N*[4](1-hydroxynaphth-2-yl)-1,4-naphthoquinone-4-imine and 5-hydroxy-dibenzo[*b*,*i*]phenazin-12(6H)-one as well as 2-amino-7-methoxy-3*H*-phenoxazin-3-one respectively. Nevertheless, there is no report concerning the reactivity of nitrosophenols towards transition-metal carbonyl clusters. In this paper, the reaction between triruthenium dodecacarbonyl and 1-nitroso-2-naphthol is described and we show that the cluster undergoes fragmentation to give two isomeric mononuclear complexes as the major products. In addition, by varying the experimental conditions, the above reaction also yields a trinuclear cluster with two co-ordinated 1,2-naphthoquinone-1-oximato moieties which adopt an unprecedented $\mu\text{-}\eta^3$-bonding mode involving the oximic oxygen atom in addition to both naphtholic oxygen and oximic nitrogen atoms. Surprisingly, we have also isolated a novel cluster with a co-ordinated phenoxazinone-like ligand which may have arisen from a 'quinone–imine or –nitrene' intermediate *via* the reductive deoxygenation of the quinone–oxime by the transition-metal carbonyl cluster.

Results and Discussion

Reaction of $[Ru_3(CO)_{12}]$ with 1-nitroso-2-naphthol

Treatment of $[Ru_3(CO)_{12}]$ with an excess of 1-nitroso-2-naphthol (Hnqo) in tetrahydrofuran (thf) afforded two orange-red products *trans*-$[Ru\{\eta^2\text{-}N(O)C_{10}H_6O\}_2(CO)_2]$ **1a** and *cis*-$[Ru\{\eta^2\text{-}N(O)C_{10}H_6O\}_2(CO)_2]$ **1b** in high yield upon TLC separation (Scheme 2). Complexes **1a** and **1b** were characterised by spectroscopic methods which revealed that they were isomeric in nature as evidenced from their very similar mass spectra. The molecular weight and the isotopic distribution of the parent ion peaks indicate that both **1a** and **1b** are mononuclear complexes with two co-ordinated nqo ligands. Their similar IR spectra with two strong bands in the region of the carbonyl absorptions are consistent with a *cis* dicarbonyl arrangement of the metal complexes.[11] In order to elucidate the structures of these complexes, the molecular structure of **1b** was established unambiguously by X-ray diffraction analysis.

The molecular structure of *cis*-$[Ru\{\eta^2\text{-}N(O)C_{10}H_6O\}_2(CO)_2]$ **1b** is depicted in Fig. 1 while selected bond parameters are given in Table 1. As shown, the molecule of **1b** contains a pseudo-octahedrally co-ordinated ruthenium centre. The two carbonyls

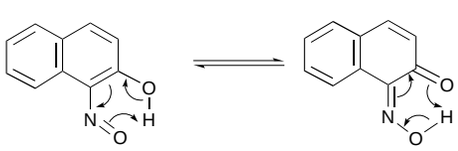

Scheme 1 Tautomerization of 1-nitroso-2-naphthol

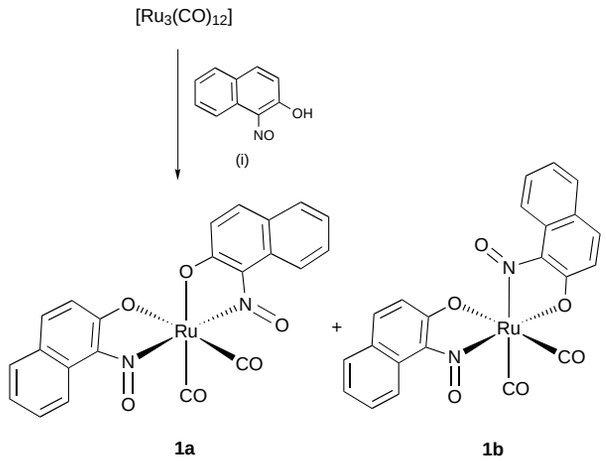

Scheme 2 (*i*) thf, room temperature (r.t.) for 3d

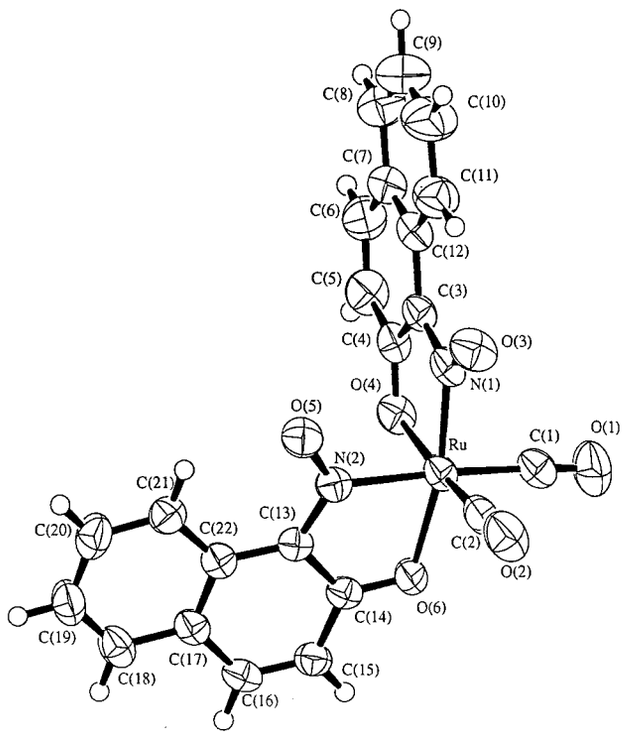

Fig. 1 The ORTEP[12] plot (50% probability) showing the molecular structure of *cis*-[Ru{η^2-N(O)$C_{10}H_6O$}$_2$(CO)$_2$] **1b** and the atom numbering scheme

adopt a *cis* configuration while the remaining co-ordination sites are occupied by the two 1,2-naphthoquinone-2-oximato (nqo) ligands with a geometry similar to that of [Ru(C_9H_6-NO)$_2$(CO)$_2$] (C_9H_6NO = quinolin-8-olate).[13] The nqo moieties act as bidentate ligands which co-ordinate to the ruthenium centre *via* the naphtholic oxygen atoms and the nitroso nitrogen atoms to form a five-membered chelated ring. The nitroso oxygen atoms are non-co-ordinating and a similar arrangement is found for those complexes with quinone–oxime type ligands.[8] The average N–O bond distance of the nitroso group is 1.257(5) Å which is within the range of most metal complexes with N-bonded nitroso groups such as [Cu{η^2-N(O)$C_{10}H_6O$}(PPh_3)$_2$] [1.287(13) Å],[8a] [Hpy][Ir{η^2-N(O)$C_{10}H_6O$}(py)Cl_3] (py = pyridine) [1.274(8) Å][8b] and [Cu{η^2-N(O)$C_{10}H_6O$}$_2$] [1.257 Å].[8c] Similar to [Ru{η^2-N(O)$C_{10}H_6O$}$_2$(py)$_2$],[8d] the two nqo ligands in **1b** are chemically different in which the two naphtholic oxygen atoms as well as the two nitroso nitrogen atoms of the two nqo groups are located *cis* to each other. The Ru–O(6) bond [2.086(3) Å] [N(1)–Ru–O(6) 167.8°] *trans* to the nitroso group is longer than the Ru–O(4) bond [2.064(3) Å] [C(2)–Ru–O(4) 173.2°] *trans* to the carbonyl group indicating that the *trans* influence of a nitroso group is stronger than that of CO. Also, the Ru–N(1) [2.005(4) Å] *trans* to the naphtholic oxygen is significantly shorter than the Ru–N(2) [2.062(4) Å] *trans* to the carbonyl. The two nqo ligands are essentially planar with maximum deviations of 0.131 and 0.144 Å. The dihedral angle between these two ligand planes is 79.8°. The angle formed by the ruthenium atom with each nqo ligand deviating significantly from 90° [N(2)–Ru–O(6) 77.8(1) and N(1)–Ru–O(4) 79.6(2)°] which is caused, primarily, by the formation of the five-membered chelate rings, as in other complexes containing nqo ligands.[8]

Table 1 Selected interatomic distances (Å) and angles (°) for complex **1b** with estimated standard deviations (e.s.d.s) in parentheses

Ru–O(4)	2.064(3)	C(6)–C(7)	1.431(8)
Ru–O(6)	2.086(3)	C(7)–C(8)	1.399(8)
Ru–N(1)	2.005(4)	C(7)–C(12)	1.402(7)
Ru–N(2)	2.062(4)	C(8)–C(9)	1.322(9)
Ru–C(1)	1.919(6)	C(9)–C(10)	1.381(9)
Ru–C(2)	1.879(6)	C(10)–C(11)	1.379(8)
O(1)–C(1)	1.125(6)	C(11)–C(12)	1.397(7)
O(2)–C(2)	1.129(6)	C(13)–C(14)	1.433(6)
O(3)–N(1)	1.258(5)	C(13)–C(22)	1.443(6)
O(4)–C(4)	1.295(6)	C(14)–C(15)	1.429(6)
O(5)–N(2)	1.256(5)	C(15)–C(16)	1.339(6)
O(6)–C(14)	1.268(5)	C(16)–C(17)	1.438(7)
N(1)–C(3)	1.363(6)	C(17)–C(18)	1.394(6)
N(2)–C(13)	1.355(6)	C(17)–C(22)	1.410(6)
C(3)–C(4)	1.411(7)	C(18)–C(19)	1.358(8)
C(3)–C(12)	1.452(7)	C(19)–C(20)	1.388(8)
C(4)–C(5)	1.418(7)	C(20)–C(21)	1.378(7)
C(5)–C(6)	1.320(8)	C(21)–C(22)	1.396(7)
O(4)–Ru–O(6)	91.5(1)	O(6)–Ru–C(2)	94.9(2)
O(4)–Ru–N(1)	79.6(2)	N(1)–Ru–N(2)	93.0(2)
O(4)–Ru–N(2)	84.8(1)	N(1)–Ru–C(1)	93.3(2)
O(4)–Ru–C(1)	91.1(2)	N(1)–Ru–C(2)	93.7(2)
O(4)–Ru–C(2)	173.2(2)	N(2)–Ru–C(1)	171.8(2)
O(6)–Ru–N(1)	167.8(1)	N(2)–Ru–C(2)	94.5(2)
O(6)–Ru–N(2)	77.8(1)	C(1)–Ru–C(2)	90.4(2)
O(6)–Ru–C(1)	95.3(2)		

Substitution reaction of complex 1a

Unfortunately, attempts to establish the molecular structure of **1a** failed as we were unable to produce single crystals from most of the commonly used organic solvent systems. From the ^{1}H NMR spectrum of **1a**, only one type of proton signal due to the nqo ligands was observed suggesting that the two co-ordinated nqo ligands are chemically equivalent, *i.e.*, complex **1a** either adopts structure **I** or **II**, see Fig. 2, but these two forms cannot be distinguished from their spectroscopic data.

To shed light on the molecular geometry of **1a**, derivatives of it were prepared. Pyridine-type ligands such as acetylpyridine were chosen and allowed to react with **1a** at room temperature. Unfortunately, no observable reaction occurred even in refluxing thf. However, when trimethylamine *N*-oxide was added, instantaneous darkening of the solution resulted. Chromatographic separation of the above reaction mixture afforded **1a** and a brown solid, *trans*-[Ru{η^2-N(O)$C_{10}H_6O$}$_2${$NC_5H_4C(O)CH_3$}(CO)] **2** (Scheme 3). Spectroscopic data suggested that complex **2** is a mono-substituted product with one carbonyl group replaced by an acetylpyridine ligand. Complex **2** is an air-stable compound that is also stable to heat and even carbonylation in refluxing $CHCl_3$. Dark brown prisms of **2** suitable for an X-ray study were obtained by slow evaporation of a cyclohexane–CH_2Cl_2 solution at −20 °C.

The molecular structure and the selected bond parameters of complex **2** are depicted in Fig. 3 and Table 2 respectively. A distorted octahedral co-ordination of the ruthenium metal centre similar to that of **1b** is observed. The molecule consists

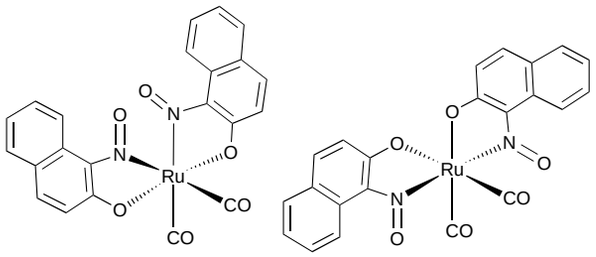

I II

Fig. 2 Two possible forms of compound **1a**

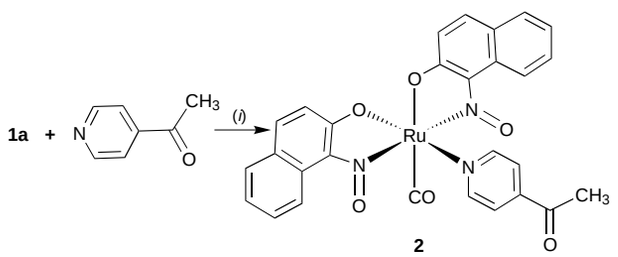

2

Scheme 3 (*i*) 1 Equivalent Me_3NO in CH_2Cl_2 at r.t.

of two nqo ligands, a co-ordinated acetylpyridine and a carbonyl group as expected in which the geometry resembles **II** rather than the other possible isomer **I**. In contrast to **1b**, the two naphtholic oxygen atoms are in the *cis* configuration [O(3)–Ru–O(5) 85.2(6)°] while the two nitroso groups are *trans* to each other [N(1)–Ru–N(2) 169.5(8)°]. The mean Ru–O distance of the naphtholic groups and the mean Ru–N distance of the nitroso groups are 2.065(1) and 2.025(2) Å respectively. The mean N–O bond distance is found to be 1.275(2) Å which is in reasonable agreement when compared with previously mentioned complexes.[8] The angles formed by the ruthenium centre with each of the nqo moieties [77.4(7) and 78.4(7)°] are comparable to those observed in **1b**. The two nqo ligands are essentially planar with a maximum deviation of 0.082 and 0.155 Å while the dihedral angle between these two ligand planes is 75.6°. Acetylpyridine is co-ordinated to the ruthenium centre *via* the nitrogen atom of the pyridine ring with a Ru–N(3) bond length of 2.09(2) Å which is consistent with the distance between the ruthenium centre and the N atom of the pyridine [2.085(4) Å] in $[Ru\{\eta^2\text{-}N(O)C_{10}H_6O\}_2(py)_2]$.[8d] The pyridyl ring itself is planar which gives dihedral angles of 89.8 and 53.6° with the nqo ligands in *cis* and *trans* positions respectively. The bonding between the ruthenium metal and the carbonyl ligand is rather short at only 1.73(3) Å while the C–O bond distance is comparatively longer [1.21(3) Å] than in **1b** [1.125(6) and 1.129(6) Å].

As compound **2** adopts the molecular geometry of structure **II**, it is conceivable that **1a** could also have the same ligand arrangement, if the formation of **2** only involved substitution of a carbonyl ligand. However, the possibility of **1a** adopting structure **I** cannot be ruled out if rearrangement of the co-ordinated nqo ligands in **1a** occurs. Therefore, a control experiment was performed under the same experimental conditions except that the acetylpyridine ligand was replaced by an excess of acetonitrile. Purification of products by chromatography yielded unreacted **1a** and a reddish brown solid which was characterised as *trans*-$[Ru\{\eta^2\text{-}N(O)C_{10}H_6O\}_2(NCMe)(CO)]$ **3** by spectroscopic means. In the ^{1}H NMR spectrum of **3**, the distributions of the proton resonances due to the two nqo ligands are almost identical to those in **2** suggesting both **2** and **3** have the same structural arrangement of the two nqo ligands around the ruthenium centre. Mass spectroscopy for the remaining reaction mixture revealed the absence of other products with molecular formulae of $[Ru(nqo)_2(CO)_2]$ and $[Ru(nqo)_2(NCMe)(CO)]$ further confirming that there is no structural rearrangement of nqo ligands during substitution.

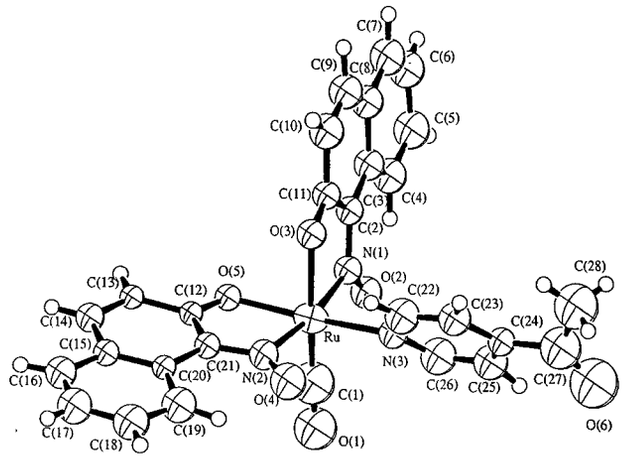

Fig. 3 The ORTEP plot (50% probability) showing the molecular structure of *trans*-$[Ru\{\eta^2\text{-}N(O)C_{10}H_6O\}_2\{NC_5H_4C(O)CH_3\}(CO)]$ **2** and the atom numbering scheme

Table 2 Selected interatomic distances (Å) and angles (°) for complex **2** with e.s.d.s in parentheses

Ru–O(3)	2.07(1)	C(6)–C(7)	1.33(3)
Ru–N(1)	2.00(2)	C(8)–C(9)	1.39(3)
Ru–N(3)	2.09(2)	C(10)–C(11)	1.46(3)
Ru–O(5)	2.06(1)	C(12)–C(21)	1.40(3)
Ru–N(2)	2.05(2)	C(14)–C(15)	1.45(3)
Ru–C(1)	1.73(3)	C(15)–C(20)	1.37(3)
O(3)–C(11)	1.27(2)	C(17)–C(18)	1.37(3)
O(5)–C(12)	1.28(2)	C(19)–C(20)	1.43(3)
N(1)–C(2)	1.34(2)	C(22)–C(23)	1.36(3)
N(3)–C(22)	1.37(3)	C(24)–C(25)	1.38(3)
O(2)–N(1)	1.27(2)	C(25)–C(26)	1.35(3)
O(4)–N(2)	1.28(2)	C(2)–C(11)	1.39(3)
O(6)–C(27)	1.22(3)	C(3)–C(8)	1.46(3)
N(2)–C(21)	1.32(2)	C(5)–C(6)	1.42(3)
N(3)–C(26)	1.37(3)	C(7)–C(8)	1.41(3)
C(1)–O(1)	1.21(3)	C(9)–C(10)	1.27(3)
C(2)–C(3)	1.44(3)	C(12)–C(13)	1.42(3)
C(3)–C(4)	1.44(3)	C(13)–C(14)	1.36(3)
C(4)–C(5)	1.37(3)	C(15)–C(16)	1.41(3)
C(16)–C(17)	1.36(3)	C(23)–C(24)	1.38(3)
C(18)–C(19)	1.43(3)	C(24)–C(27)	1.50(4)
C(20)–C(21)	1.48(3)	C(27)–C(28)	1.43(4)
O(3)–Ru–O(5)	85.2(6)	O(3)–Ru–N(1)	78.4(7)
O(3)–Ru–N(2)	93.9(7)	O(3)–Ru–N(3)	89.1(7)
O(3)–Ru–C(1)	171(1)	O(5)–Ru–N(1)	94.7(7)
O(5)–Ru–N(2)	77.4(1)	O(5)–Ru–N(3)	172.4(8)
O(5)–Ru–C(1)	93(1)	N(1)–Ru–N(2)	169.5(8)
N(1)–Ru–N(3)	89.0(7)	N(1)–Ru–C(1)	93(1)
N(2)–Ru–N(3)	98.0(8)	N(2)–Ru–C(1)	93(1)
N(3)–Ru–C(1)	92(1)		

Reactivity of compounds 1a and 1b

Both **1a** and **1b** are thermally stable up to the refluxing temperature of $CHCl_3$ and thf without any molecular rearrangement or decomposition. Acidification of **1a** in deuteriated chloroform using trifluoroacetic acid, CF_3CO_2H, resulted in a slight darkening of colour. Monitoring of the reaction mixture by both ^{1}H NMR spectroscopy and spot TLC showed no observable change even in a thermostat for 3 d at 65 °C. However, when CF_3CO_2H was added to a NMR tube containing **1b** in CD_2Cl_2, a change in the proton NMR spectrum was observed after warming the sample at 30 °C for 1 h. The reaction mixture was continuously monitored by ^{1}H NMR spectroscopy which showed that proton resonances due to **1b** gradually decreased accompanied by an increase in intensities of other proton sig-

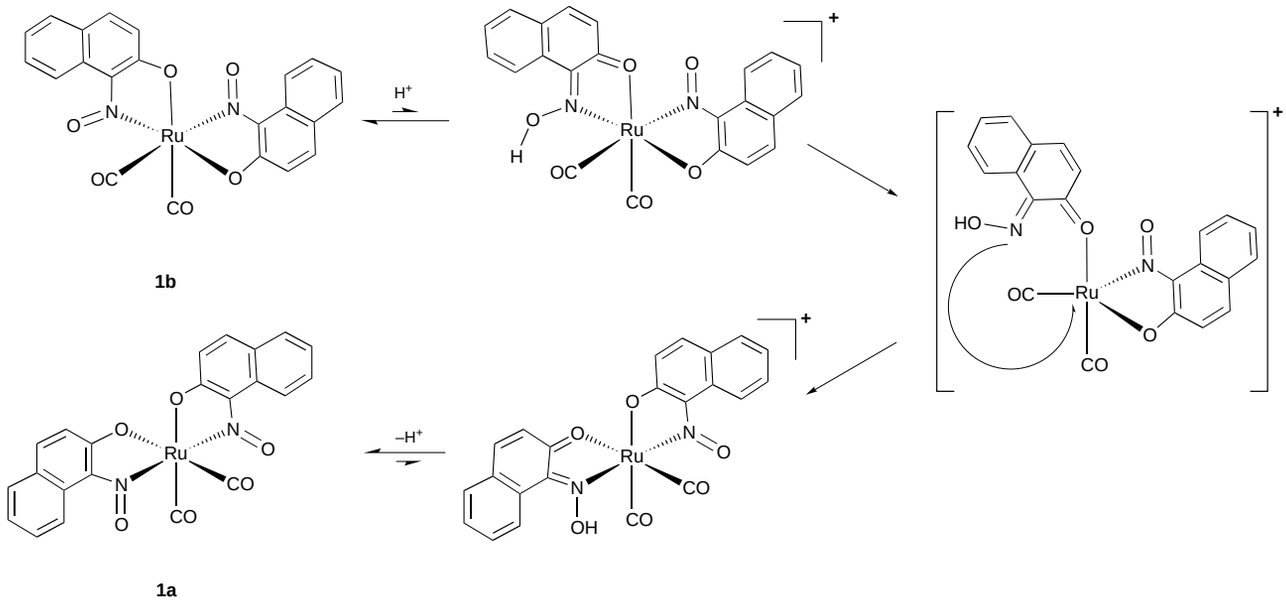

Scheme 4 A proposed mechanism for the acid catalysed isomerisation of compound **1b** to **1a**

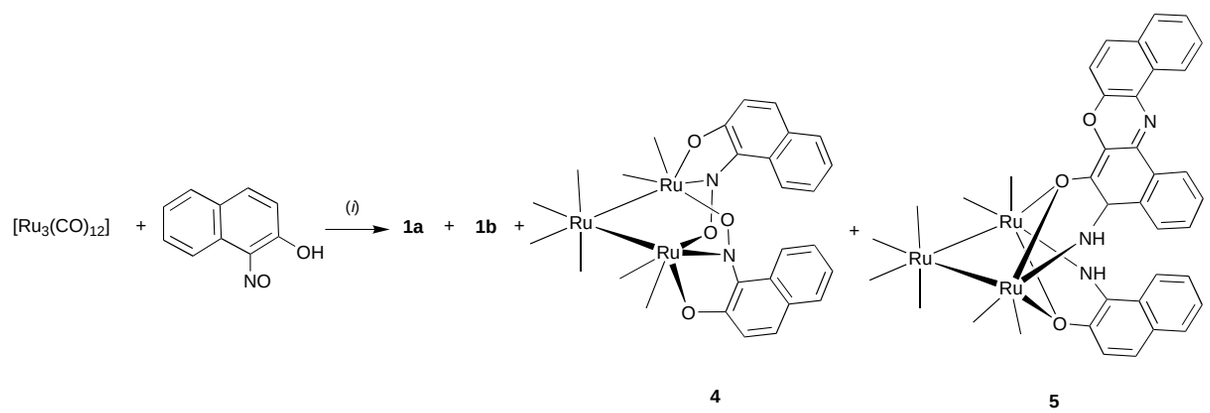

Scheme 5 (*i*) Refluxing thf for 1 h

nals. The proton resonances of **1b** completely disappeared after 1 d. A single product **1a**, was formed and its identity was confirmed by both ^{1}H NMR spectroscopy and its chromatographic properties. This acid-catalysed transformation of **1b** to **1a** was found to be sensitive to both temperature and the amount of acid added. A substantial increase in either of these two parameters resulted in a faster conversion rate of **1b** to **1a**. Protonation of the nitroso moieties to give oximes is found to be a reversible process with a higher tendency towards the backward reaction to give the nitroso group rather than the forward reaction to form the unstable oxime moieties. This is supported by both IR and ^{1}H NMR spectroscopy in which no signals attributable to the protonated species can be observed. Therefore, increasing the amount of trifluoroacetic acid would shift the equilibrium towards the formation of the oxime and suppress the backward reaction. As a result, a plausible mechanism can be proposed for the conversion of **1b** to **1a** (Scheme 4).

Reaction of $[Ru_3(CO)_{12}]$ with Hnqo at high temperature

The reaction of $[Ru_3(CO)_{12}]$ and excess of 1-nitroso-2-naphthol was carried out in refluxing thf until all the ligand was consumed as monitored by spot TLC. In addition to **1a** and **1b**, two dark blue products $[Ru_3(\mu\text{-}\eta^3\text{-}ONC_{10}H_6O)_2(CO)_8]$ **4** and $[Ru_3\{\mu\text{-}\eta^2\text{-}N(H)C_{10}H_6O\}\{\mu\text{-}\eta^2\text{-}N(H)C_{10}H_4(O)NOC_{10}H_6\}(CO)_8]$ **5** were also isolated in low yield (Scheme 5).

We have shown that varying the stoichiometric ratio of the reactants could not improve the yield of **4** and **5** since fragmentation of the trinuclear cluster into mononuclear species was always a competing reaction. The mass spectrum of complex **4** was consistent with a triruthenium carbonyl cluster containing two Hnqo moieties. Infrared spectroscopy indicated that cluster **4** should contain terminal carbonyls while only one set of proton resonance signals due to the Hnqo ligand was observed in the ^{1}H NMR spectrum. The molecular structure of cluster **4** was established by X-ray analysis using a dark blue, air stable crystal which was obtained by the diffusion of diethyl ether into a dichloromethane solution at −20 °C. Fig. 4 shows the perspective view and the numbering scheme for the resulting molecular configuration. Selected bond parameters are given in Table 3. The cluster consists of an open Ru_3 triangle with two nqo ligands spanning the open Ru · · · Ru edge [3.503(1) Å] *via* the nitroso groups in a $\mu\text{-}\eta^2$-fashion and is similar to the recently characterised cluster $[Ru_3(\mu_3\text{-}NPh)_2(\mu\text{-}\eta^2\text{-}ONPh)_2(CO)_7]$.[4] The two metal–metal bond distances are almost equal [Ru(1)–Ru(2) 2.794(2) and Ru(2)–Ru(3) 2.805(2) Å]. The two co-ordinated nqo moieties are essentially planar with maximum deviations of 0.15 and 0.18 Å from their idealised plane. In contrast to compounds **1b** and **2**, the nqo ligands are chelated to the metal core in a $\mu\text{-}\eta^3$-manner by means of the naphtholic oxygen atoms [mean Ru–O 2.210(1) Å], nitroso nitrogen atoms [mean Ru–N 2.115(1) Å] and nitroso oxygen atoms [mean Ru–O 2.135(1) Å]. The former two atoms are chelated to the same metal centre to give a five-membered ring similar to those of mononuclear complexes, **1b** and **2**. In addition, the nitroso oxygen atoms span to the neighbouring metal centre over the

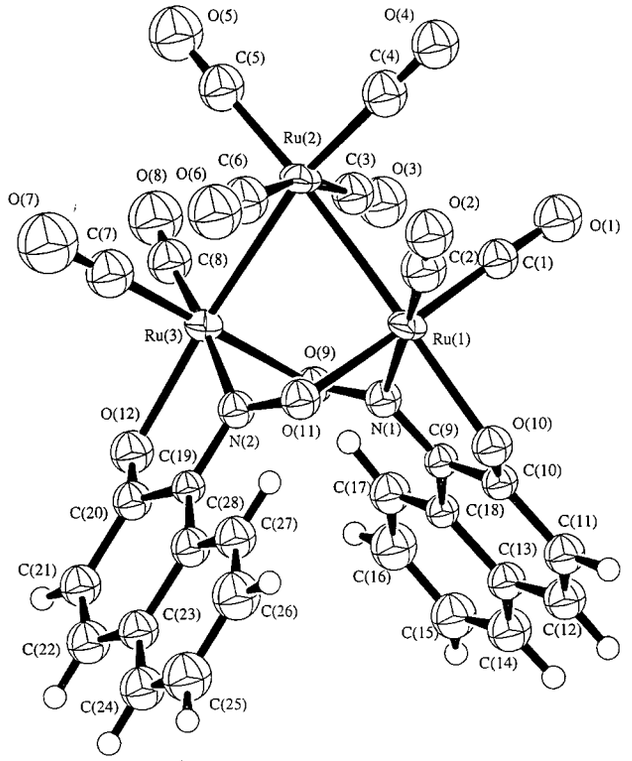

Fig. 4 The ORTEP plot (50% probability) showing the molecular structure of $[Ru_3(\mu\text{-}\eta^3\text{-}ONC_{10}H_6O)_2(CO)_8]$ **4** and the atom numbering scheme

Table 3 Selected interatomic distances (Å) and angles (°) for cluster **4** with e.s.d.s in parentheses

Ru(1)–Ru(2)	2.794(2)	Ru(1)–O(10)	2.22(1)
Ru(2)–Ru(3)	2.805(2)	Ru(1)–N(1)	2.14(1)
Ru(1)–O(11)	2.13(1)	Ru(3)–O(9)	2.14(1)
Ru(3)–O(12)	2.20(1)	Ru(3)–N(2)	2.09(1)
N(1)–O(9)	1.30(1)	O(12)–C(20)	1.20(2)
N(2)–O(11)	1.31(1)	N(2)–C(19)	1.38(2)
N(1)–C(9)	1.33(2)	C(9)–C(18)	1.51(2)
C(9)–C(10)	1.43(2)	C(11)–C(12)	1.34(2)
C(10)–C(11)	1.46(2)	C(12)–C(13)	1.42(2)
C(13)–C(18)	1.44(2)	C(13)–C(14)	1.39(2)
C(19)–C(28)	1.42(2)	C(14)–C(15)	1.38(2)
C(20)–C(21)	1.48(2)	C(15)–C(16)	1.39(2)
C(21)–C(22)	1.34(2)	C(16)–C(17)	1.41(2)
C(22)–C(23)	1.39(2)	C(17)–C(18)	1.36(2)
C(23)–C(24)	1.41(2)	C(19)–C(20)	1.47(2)
C(24)–C(25)	1.34(2)	C(23)–C(28)	1.47(2)
C(25)–C(26)	1.44(2)	C(27)–C(28)	1.38(2)
C(26)–C(27)	1.35(2)		
Ru(1)–Ru(2)–Ru(3)	77.46(6)	Ru(2)–Ru(1)–O(11)	93.3(3)
Ru(2)–Ru(1)–O(10)	167.9(3)	O(10)–Ru(1)–O(11)	90.5(4)
Ru(2)–Ru(1)–N(1)	95.1(3)	O(11)–Ru(1)–N(1)	86.2(4)
O(10)–Ru(1)–N(1)	73.7(4)	Ru(1)–N(1)–O(9)	123.3(9)
Ru(1)–O(11)–N(2)	113.1(9)	Ru(3)–O(9)–N(1)	116.6(8)
Ru(3)–N(2)–O(11)	126(1)		

open metal–metal edge. The N–O bond distances [mean 1.305(1) Å] are significantly longer than those found for N-bonded nitroso groups [mean 1.257(5) Å for **1b** and 1.275(2) Å for **2**] but are comparably shorter than those complexes with μ-η^2-co-ordinated nitroso moieties such as $[Fe_2(\mu\text{-}\eta^2\text{-}ONCMe_2)(\mu\text{-}NHCHMe_2)(CO)_6]$ [1.371(5) Å][14] and $[Fe_2(\mu\text{-}\eta^2\text{-}ONCMe_2)(\mu\text{-}NCMe_2)(CO)_6]$ [1.351(6) Å].[15] The nqo ligands in **4** act as an unprecedented $5e^-$ donor rather than a $3e^-$ donor as in the case for both **1b** and **2**. Together with the eight terminal carbonyls, cluster **4** is electron precise with a cluster valence electron (CVE) count of 50 which is expected for a trinuclear cluster with two metal–metal bonds.

From the structural point of view, it is reasonable to assume that the interaction between Hnqo and $[Ru_3(CO)_{12}]$ should involve the formation of a triruthenium cluster with co-ordinated Hnqo ligands followed by metal–metal bond cleavage in the presence of an excess of ligand to form the mononuclear species **1a** and **1b**. Thus, cluster **4** is suspected to be an intermediate in the formation of **1a** and **1b**. However, the reaction between cluster **4** and an excess of Hnqo resulted only in decomposition of **4**. On the other hand, cluster **4** could only be isolated when the reaction of $[Ru_3(CO)_{12}]$ with Hnqo was performed at higher temperature. At 0 °C, no cluster **4** can be obtained and also the reaction proceeds at a much slower rate. Therefore, the formation of cluster **4** must involve another reaction pathway.

Apart from cluster **4**, another minor product, $[Ru_3\{\mu\text{-}\eta^2\text{-}N(H)C_{10}H_6O\}\{\mu\text{-}\eta^2\text{-}N(H)C_{10}H_4(O)NOC_{10}H_6\}(CO)_8]$ **5** could also be isolated from the same reaction mixture. Compound **5** has been characterised spectroscopically (mass, IR AND ^{1}H NMR). The mass spectrum of **5** exhibits a peak envelope at *m*/*z* 996 with an isotopic pattern corresponding to three ruthenium atoms while IR spectroscopy shows the presence of terminal carbonyls only. The ^{1}H NMR spectrum of **5** is very complicated and consists of proton signals ranging from δ 3.5 to 9.0. However, no metal hydride could be detected. In order to elucidate the structure of **5**, dark blue crystals of stoichiometry $\mathbf{5}\cdot CH_2Cl_2\cdot MeOH$ were grown from a solution mixture of methanol and CH_2Cl_2 at −20 °C. A perspective view of the molecular structure of **5** together with the atomic numbering scheme is illustrated in Fig. 5(*a*). Selected bond lengths and angles are listed in Table 4. Knowledge of the solid-state structure of **5** allows the solution spectroscopic data, particularly the ^{1}H NMR spectrum, to be interpreted. The proton resonances between δ 6.9 and 9.0 are due to the aromatic ring system while the two broad peaks at δ 4.87 and 3.56 are attributable to the N–H of the two imine groups. The molecule consists of an open triangular array of three ruthenium atoms with two different kinds of quinone–imine ligands bridging the open Ru · · · Ru edge, similar to the geometry of $[Ru_3(\mu\text{-}\eta^2\text{-}NC_9H_6O)_2(CO)_8]$ reported by van Doorn and van Leeuwen[13] from the reaction between $[Ru_3(CO)_{12}]$ and quinolin-8-ol. The two Ru–Ru bonds are approximately equal [2.751(2) *vs.* 2.747(2) Å] while the Ru(1) · · · R(2) edge is non-bonded with an atomic separation of 3.040(1) Å. This non-bonded Ru · · · Ru vector is bridged by two different quinone–imine moieties, $N(H)C_{10}H_6O$ and $N(H)C_{10}H_4(O)NOC_{10}H_6$ *via* a μ-η^2-fashion in which both naphtholic oxygen atoms and imido nitrogen atoms are co-ordinated on the same ruthenium centre forming a five-membered chelate ring with mean Ru–O and Ru–N distances of 2.136(10) and 2.183(9) Å. The naphtholic oxygen is also bonded to the neighbouring Ru atom asymmetrically [mean Ru–O 2.209(9) Å] over the open Ru · · · Ru edge. The two phenyl rings, C(11)–C(12)–C(13)–C(14)–C(15)–C(16) and C(31)–C(36)–C(35)–C(34)–C(33)–C(32) of the two macrocycles are cofacially overlapped with a dihedral angle of 19.4° between these two planes as shown in Fig. 5(*b*). Each quinone–imine ligand itself should be a five-electron donor with the μ-bridging naphtholic oxygen and imido nitrogen atom contributing two and three electrons respectively to the cluster framework. Together with the eight terminal carbonyls, cluster **5** is electron precise for a triruthenium carbonyl cluster with two Ru–Ru bonds in accordance to the effective atomic number (EAN) rule.

The two different naphthoquinone–imine type ligands arise from the deoxygenation of a Hnqo ligand in the presence of $[Ru_3(CO)_{12}]$ to give a naphthoquinone–imine or –nitrene intermediate.[16] This unstable intermediate will further react with an excess of $[Ru_3(CO)_{12}]$ to form a co-ordinated cluster species with the oxygen atom of the naphthoquinone and the imine nitrogen atom chelated to a ruthenium atom forming a five-membered ring similar to the co-ordination geometry of most quinone–oxime ligands. The oxygen atom of the co-ordinated

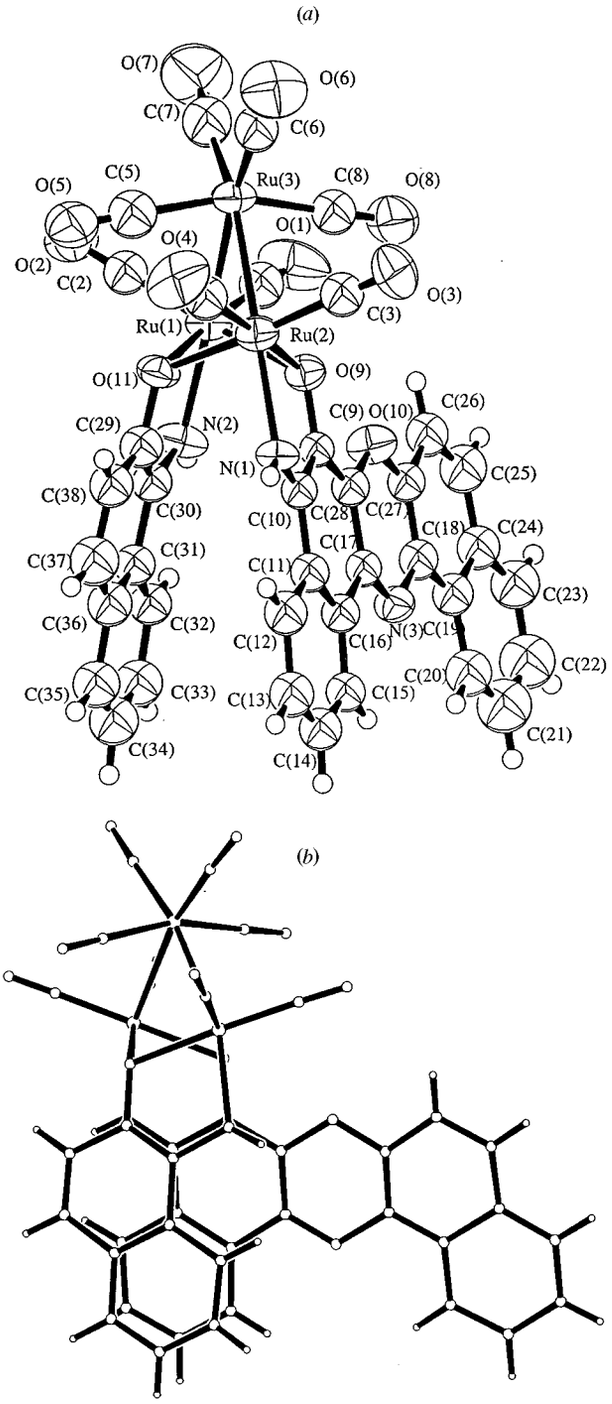

Fig. 5 (*a*) The ORTEP plot (50% probability) showing the molecular structure of $[Ru_3\{\mu\text{-}\eta^2\text{-}N(H)C_{10}H_6O\}\{\mu\text{-}\eta^2\text{-}N(H)C_{10}H_4(O)NOC_{10}H_6\}(CO)_8]$ **5** and the atom numbering scheme; (*b*) front and side views of **5** illustrating the orientation of the two π systems

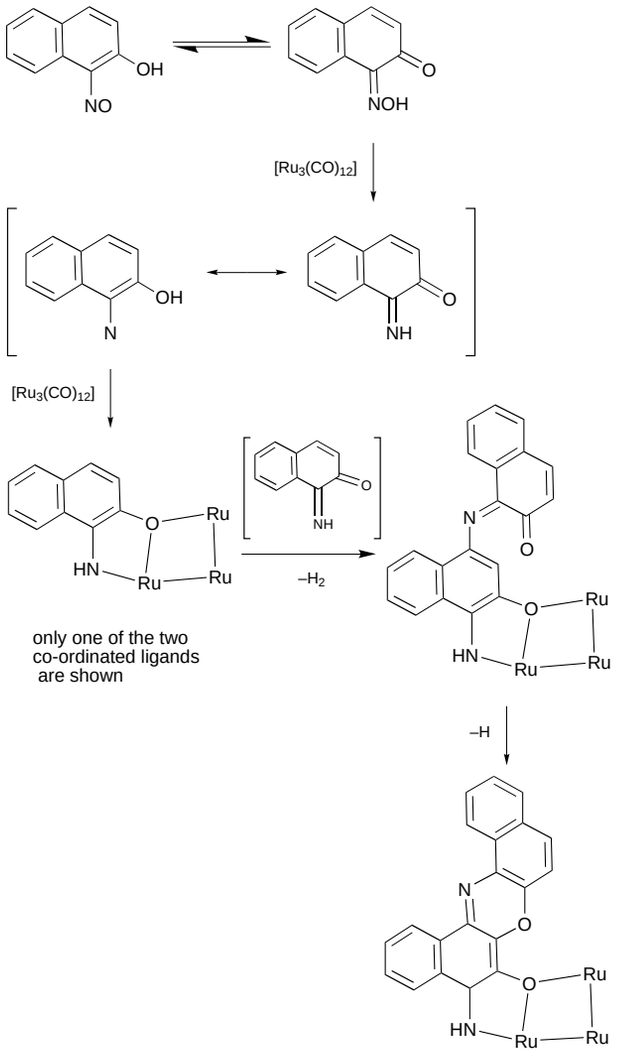

Scheme 6 A proposed mechanism for the formation of the phenoxazinone moiety through the quinone–imine intermediate in cluster **5**

naphthoquinone–imine bridges to the neighbouring ruthenium atom followed by metal–metal bond cleavage to form a $\mu\text{-}\eta^2$-co-ordinated 1,2-naphthoquinone-1-imine ligand. Surprisingly, there is another quinone–imine type ligand with an extensive conjugated π system consisting of five six-membered rings arranged in a planar fashion (maximum deviation 0.17 Å). This unusual ring system is composed of two naphthalene subunits which are linked together by two heteroatoms, N and O, similar to the skeleton of phenoxazin-2-one[16] rather than phenoxazine as no proton signals attributed to the N–H can be observed. According to Buckley *et al.*,[8a,17] the formation of this ligand should involve coupling reactions between an extra naphthoquinone–imine or –nitrene intermediate and the co-ordinated naphthoquinone–imine ligand with the former species attacking the 4-position followed by ring closure as shown in Scheme 6. According to the proposed mechanism, a stable intermediate with two 1,2-naphthoquinone-1-imine ligands chelated on a triruthenium core in a $\mu\text{-}\eta^2$-co-ordination mode should exist in order to give cluster **5**. However, this suspected precursor cannot be obtained which may be due to unfavourable experimental conditions for its isolation. Nevertheless, attempts to quench such intermediates are currently in progress.

Experimental

General procedures

All manipulations were carried out under an inert atmosphere of argon with standard Schlenk techniques, unless stated otherwise. Commercial chemicals such as triruthenium dodecacarbonyl (Strem), 1-nitroso-2-naphthol (Lancaster), trifluoroacetic acid (Aldrich) and acetylpyridine (Aldrich) were used directly as received. Trimethylamine *N*-oxide (Aldrich) was dried by azeotropic distillation and sublimed prior to use. Dichloromethane, chloroform and acetonitrile were distilled from CaH_2 while thf, *n*-hexane and toluene were distilled from sodium benzophenone under N_2. Preparative thin-layer chromatographic (TLC) plates were prepared from silica (Merck Kieselgel 60 GF_{254}). Infrared spectra were recorded on a Biorad FTS-165 FT-IR spectrometer using 0.5 mm CaF_2 solution cells, ^{1}H NMR spectra were obtained on a Bruker DPX-300

Table 4 Selected interatomic distances (Å) and angles (°) for cluster **5** with e.s.d.s in parentheses

Ru(1)–Ru(3)	2.751(2)	C(11)–C(16)	1.43(2)
Ru(2)–Ru(3)	2.747(2)	C(15)–C(16)	1.39(2)
Ru(1)–O(11)	2.127(10)	C(17)–C(28)	1.43(2)
Ru(2)–O(11)	2.206(9)	C(18)–C(27)	1.37(2)
Ru(1)–O(9)	2.211(9)	C(19)–C(20)	1.42(2)
Ru(1)–N(2)	2.20(1)	C(20)–C(21)	1.42(3)
Ru(2)–O(9)	2.136(10)	C(21)–C(22)	1.40(3)
Ru(2)–N(1)	2.183(9)	C(22)–C(23)	1.38(2)
O(9)–C(9)	1.36(1)	C(23)–C(24)	1.40(2)
O(11)–C(29)	1.35(2)	C(24)–C(25)	1.41(2)
O(10)–C(27)	1.36(2)	C(25)–C(26)	1.35(2)
O(10)–C(28)	1.39(2)	C(26)–C(27)	1.43(2)
N(3)–C(17)	1.30(2)	C(19)–C(24)	1.48(2)
N(3)–C(18)	1.42(2)	C(29)–C(30)	1.32(2)
N(1)–C(10)	1.21(2)	C(29)–C(38)	1.43(2)
N(2)–C(30)	1.44(2)	C(31)–C(36)	1.41(2)
C(9)–C(28)	1.38(2)	C(30)–C(31)	1.47(2)
C(11)–C(12)	1.42(2)	C(31)–C(32)	1.42(2)
C(12)–C(13)	1.44(2)	C(32)–C(33)	1.41(2)
C(14)–C(15)	1.32(2)	C(33)–C(34)	1.39(2)
C(16)–C(17)	1.47(2)	C(34)–C(35)	1.33(2)
C(18)–C(19)	1.38(2)	C(35)–C(36)	1.44(2)
C(10)–C(11)	1.44(2)	C(36)–C(37)	1.43(2)
C(13)–C(14)	1.36(2)	C(37)–C(38)	1.36(2)
Ru(1)–Ru(3)–Ru(2)	67.13(4)	Ru(3)–Ru(1)–O(11)	84.6(2)
Ru(3)–Ru(1)–O(9)	84.0(2)	O(9)–Ru(1)–O(11)	77.3(4)
Ru(3)–Ru(1)–N(2)	162.5(3)	O(11)–Ru(1)–N(2)	78.4(4)
O(9)–Ru(1)–N(2)	88.3(4)	Ru(3)–Ru(2)–O(9)	85.5(2)
Ru(3)–Ru(2)–O(11)	83.3(2)	Ru(3)–Ru(2)–N(1)	161.3(3)
O(9)–Ru(2)–O(11)	77.2(4)	O(9)–Ru(2)–N(1)	77.1(4)
O(11)–Ru(2)–N(1)	86.2(4)	Ru(1)–O(9)–Ru(2)	88.7(3)
Ru(1)–O(11)–Ru(2)	89.1(3)	C(27)–O(10)–C(28)	116(1)
C(17)–N(3)–C(18)	117(1)		

NMR spectrometer using deuteriated solvents as lock and reference. Fast atom bombardment (FAB) mass spectra were recorded on a Finnigan MAT 95 mass spectrometer. Elemental analyses were performed by Butterworth Laboratories Ltd., UK.

Reaction of $[Ru_3(CO)_{12}]$ with 1-nitroso-2-naphthol

The compounds $[Ru_3(CO)_{12}]$ (639 mg, 1.0 mmol) and 1-nitroso-2-naphthol (346 mg, 2.0 mmol) were dissolved in thf (60 cm^3). The colour of the solution changed from dark orange to dark reddish brown. After stirring for 3 d at room temperature, the solvent was removed *in vacuo*. The residue was extracted with dichloromethane, and the extract was filtered and chromatographed by preparative TLC on silica gel. Elution with *n*-hexane–CH_2Cl_2 (1:1, v/v) resolved three bands. The first yellow band was the unreacted $[Ru_3(CO)_{12}]$ (256 mg, 40%) followed by two intense orange bands with R_f 0.5 and 0.4 which were isolated and characterised as *trans*-$[Ru\{\eta^2\text{-}N(O)C_{10}H_6O\}_2(CO)_2]$ **1a** (225 mg, 25%) and *cis*-$[Ru\{\eta^2\text{-}N(O)C_{10}H_6O\}_2(CO)_2]$ **1b** (271 mg, 30%) respectively based on consumed $[Ru_3(CO)_{12}]$. Orange-red rectangular crystals of **1b**·CH_2Cl_2 were obtained by slow evaporation of *n*-hexane–CH_2Cl_2 solution at −20 °C.

Data for **1a** (Found: C, 52.80; H, 2.25; N, 5.45. Calc. for $C_{22}H_{12}N_2O_6Ru$: C, 52.70; H, 2.40; N, 5.60%; IR(CH_2Cl_2): 2076vs and 2022vs cm^{-1} (ν_{CO}); FAB mass spectrum: *m*/*z* 501 (M^+, ^{101}Ru); ^1H NMR (CD_2Cl_2): δ 9.14 (d, 2 H, J_{HH} = 8.0), 7.79 (d, 2 H, J_{HH} = 9.4), 7.65 (m, 4 H), 7.47 (t, 2 H, J_{HH} = 7.5) and 7.00 (d, 2 H, J_{HH} = 9.4 Hz).

Data for **1b** (Found: C, 52.70; H, 2.35; N, 5.70. Calc. for $C_{22}H_{12}N_2O_6Ru$: C, 52.70; H, 2.40; N, 5.60%); IR(CH_2Cl_2): 2077vs and 2023vs cm^{-1} (ν_{CO}); FAB mass spectrum: *m*/*z* 501 (M^+, ^{101}Ru); ^1H NMR (CD_2Cl_2): δ 9.14 (d, 1 H, J_{HH} = 8.4), 9.10 (d, 1 H, J_{HH} = 8.4), 7.77 (t, 2 H, J_{HH} = 9.2), 7.45 (m, 6 H), 7.12 (d, 1 H, J_{HH} = 9.1) and 6.94 (d, 1 H, J_{HH} = 9.1 Hz).

Reaction of compound 1a with acetylpyridine

A solution of **1a** (50 mg, 0.1 mmol) and a ten-fold excess of 4-acetylpyridine in CH_2Cl_2 was stirred at room temperature. To this dark orange solution, a CH_2Cl_2 solution (10 cm^3) of Me_3NO (7.5 mg, 0.1 mmol) was added dropwise to give a dark purple solution. After stirring for 2 h, the solvent was removed *in vacuo*. The residue was then subjected to TLC separation using *n*-hexane–CH_2Cl_2 (3:7, v/v) as eluent. Three bands were obtained in order of elution as **1a** (5 mg, 10%), *trans*-$[Ru\{\eta^2\text{-}N(O)C_{10}H_6O\}_2\{NC_5H_4C(O)CH_3\}(CO)]$ **2** (35.6 mg, 60%) and an excess of acetylpyridine. Dark brown crystals of **2**·CH_2Cl_2 were grown by slow evaporation of a solution of cyclohexane–CH_2Cl_2 at −20 °C.

Data for **2** (Found: C, 56.70; H, 3.30; N, 7.20. Calc. for $C_{28}H_{19}N_3O_6Ru$: C, 56.60; H, 3.20; N, 7.10%) IR(CH_2Cl_2): 1994vs cm^{-1} (ν_{CO}); FAB mass spectrum: *m*/*z* 594 (M^+, ^{101}Ru); ^1H NMR (CD_2Cl_2): δ 9.33 (d, 1 H, J_{HH} = 7.8), 9.21 (d, 1 H, J_{HH} = 8.2), 8.74 (d, 2 H, J_{HH} = 5.2), 7.67 (m, 8 H), 7.48 (t, 1 H, J_{HH} = 7.5), 7.39 (d, 1 H, J_{HH} = 7.5), 7.04 (d, 1 H, J_{HH} = 9.4), 6.98 (d, 1 H, J_{HH} = 9.4 Hz) and 2.58 (s, 3 H).

Thermolysis of compounds 1a and 1b

Solid samples of either compounds **1a** or **1b** were dissolved in different organic solvents such as $CHCl_3$, thf, benzene or toluene. These solutions were allowed to heat under reflux for at least 3 h. In all these cases, no observable changes were detected but slight decomposition of starting material resulted in solvents with high boiling-points.

Attempted protonation of compound 1a

To an oven-dried NMR tube inside a glovebag under argon, **1a** (5 mg, 0.01 mmol) and $CDCl_3$ (1 cm^3) were added. After all of **1a** was dissolved, an excess of trifluoroacetic acid, CF_3CO_2H, was injected by a syringe. The mixture became slightly darker and the tube was then warmed inside a thermostat at 65 °C for 3 d. Proton NMR monitoring revealed the presence of **1a** only.

Acid-catalysed isomerisation of compound 1b

Compound **1b** (5 mg, 0.01 mmol) and CD_2Cl_2 (1 cm^3) were placed in an oven-dried NMR tube under argon in a glovebag. An excess of trifluoroacetic acid was added to the orange solution *via* a syringe through the rubber serum stopper, resulting in a momentary deepening of colour. The tube was then removed from the glovebag. After warming the tube in a thermostat at 30 °C for 1 h, an ^1H NMR spectrum was recorded at time intervals of 1 h until no **1b** was detected. After 20 h, all **1b** had been converted to **1a** on the basis of ^1H NMR data.

Reaction of compound 1a with MeCN

A solid sample of **1a** (50 mg, 0.1 mmol) was dissolved in a solution of CH_2Cl_2 (40 cm^3) and MeCN (5 cm^3). To this orange solution, a CH_2Cl_2 solution (10 cm^3) of Me_3NO (7.5 mg, 0.1 mmol) was added dropwise at room temperature. The resultant dark red solution was allowed to stir for 1 h. After removal of the solvent *in vacuo*, the residue was chromatographed on TLC using CH_2Cl_2 as eluent. The first fraction was an orange band of **1a** (5 mg) followed by a reddish-brown band of *trans*-$[Ru\{\eta^2\text{-}N(O)C_{10}H_6O\}_2(NCMe)(CO)]$ **3** (31 mg, 60%).

Data for **3** (Found: C, 53.80; H, 2.95; N, 8.30. Calc. for $C_{23}H_{15}N_3O_5Ru$: C, 53.70; H, 2.90; N, 8.20%); IR(CH_2Cl_2): 1997vs cm^{-1} (ν_{CO}); FAB mass spectrum: *m*/*z* 514 (M^+, ^{101}Ru); ^1H NMR (CD_2Cl_2): δ 9.25 (d, 1 H, J_{HH} = 8.4), 9.21 (d, 1 H, J_{HH} = 8.4), 7.77 (d, 1 H, J_{HH} = 9.4), 7.69 (d, 1 H, J_{HH} = 9.4), 7.66 (m, 4 H), 7.45 (m, 2 H), 7.04 (d, 1 H, J_{HH} = 9.4), 6.98 (d, 1 H, J_{HH} = 9.4 Hz) and 2.38 (s, 3 H).

Preparation of clusters 4 and 5

The compounds $[Ru_3(CO)_{12}]$ (639 mg, 1.0 mmol) and 1-

Table 5 Summary of crystallographic parameters for complexes **1b**, **2**, **4** and **5**

	1b	**2**	**4**	**5**
Formula	$C_{22}H_{12}N_2O_6Ru\cdot CH_2Cl_2$	$C_{28}H_{19}N_3O_6Ru\cdot CH_2Cl_2$	$C_{28}H_{12}N_2O_{12}Ru_3$	$C_{38}H_{19}N_3O_{11}Ru_3\cdot CH_2Cl_2\cdot MeOH$
M	501.17	594.23	871.31	996.37
Crystal system	Triclinic	Triclinic	Monoclinic	Triclinic
Space group	$P\bar{1}$ (no. 2)	$P\bar{1}$ (no. 2)	$P2_1/n$ (no. 14)	$P\bar{1}$ (no. 2)
a/Å	7.170(1)	10.067(1)	12.482(5)	11.926(1)
b/Å	12.288(1)	12.461(1)	14.781(3)	12.217(1)
c/Å	14.168(2)	13.783(1)	16.024(5)	16.759(1)
α/°	66.73(2)	112.52(2)	90	102.72(2)
β/°	88.76(2)	106.09(2)	104.93(3)	108.79(2)
γ/°	84.17(2)	103.34(2)	90	101.02
U/Å^3	1135.8(2)	1419.8(6)	2856(1)	2162.2(7)
Z	2	2	4	2
D_c/g cm^{-3}	1.714	1.589	2.026	1.709
μ(Mo-Kα)	9.69	7.88	16.36	12.21
Diffractometer	Rigaku-AFC7R	Rigaku-AFC7R	Rigaku-AFC7R	MAR research Image Plate
No. reflections measured	3255	2890	4113	28 437
No. unique reflections	2967	1818	3909	5465
No. reflections with $I > 3\sigma(I)$	2317	1048	1975	3312
No. variables	302	180	196	336
R[a]	0.302	0.080	0.051	0.073
R'[b]	0.031	0.082	0.047	0.087
Largest Δ/σ	0.05	0.03	0.03	0.06
Residual electron density/e Å^{-3}	0.76 to −0.58	0.75 to −0.54	0.52 to −0.56	1.28 to −0.74

[a] $R = \Sigma||F_o| - |F_c||/\Sigma|F_o|$. [b] $R' = [\Sigma w(|F_o| - |F_c|)^2/\Sigma w(F_o)^2]^{\frac{1}{2}}$ where $w = [\sigma^2(F_o)]^{-1}$.

nitroso-2-naphthol (346 mg, 1.0 mmol) were dissolved in thf (70 cm^3). The dark orange solution was refluxed for 1 h to give a dark brown solution. The solvent was removed *in vacuo* and the residue was extracted with dichloromethane. The extract was filtered and chromatographed by TLC using a mixture of *n*-hexane–CH_2Cl_2 (4:6, v/v) as eluent. Five distinctive bands were observed in order of elution as $[Ru_3(CO)_{12}]$ (64 mg, 10%), $[Ru_3\{\mu\text{-}\eta^2\text{-}N(H)C_{10}H_6O\}\{\mu\text{-}\eta^2\text{-}N(H)C_{10}H_4(O)NOC_{10}H_6\}(CO)_8]$ **5** (45 mg, 5%), **1a** (271 mg, 20%), **1b** (338 mg, 25%), $[Ru_3(\mu\text{-}\eta^3\text{-}ONC_{10}H_6O)_2(CO)_8]$ **4** (24 mg, 3%) based on consumed $[Ru_3(CO)_{12}]$. Dark blue crystals of **4** and **5** suitable for X-ray diffraction analyses were grown by diffusion of diethyl ether into a CH_2Cl_2 solution and slow evaporation of a methanol–CH_2Cl_2 solution at −20 °C respectively.

Data for **4** (Found: C, 38.80; H, 1.40; N, 3.35. Calc. for $C_{28}H_{12}N_2O_{12}Ru_3$: C, 38.60; H, 1.40; N, 3.20%); IR(*n*-hexane): 2080s, 2066w, 2018vs, 2007sh, 1951m and 1724br cm^{-1} (ν_{CO}); FAB mass spectrum: *m*/*z* 871 (M^+, ^{101}Ru); ^{1}H NMR (CD_2Cl_2): δ 9.20 (d, 2 H, J_{HH} = 8.7), 7.62 (m, 4 H), 7.49 (m, 4 H) and 6.69 (d, 2 H, J_{HH} = 9.6 Hz).

Data for **5** (Found: C, 45.95; H, 2.00; N, 4.25. Calc. for $C_{38}H_{19}N_3O_{11}Ru_3$: C, 45.80; H, 1.90; N, 4.20%); IR(*n*-hexane): 2159w, 2128w, 2089m, 2059w, 2010s and 1931m cm^{-1} (ν_{CO}); FAB mass spectrum: *m*/*z* 996 (M^+, ^{101}Ru); ^{1}H NMR (CD_2Cl_2): δ 8.95 (d, 1 H, J_{HH} = 8.3), 8.47 (d, 1 H, J_{HH} = 7.5), 8.09 (d, 1 H, J_{HH} = 8.9), 7.96 (d, 1 H, J_{HH} = 8.1), 7.78 (d, 1 H, J_{HH} = 9.0), 7.77 (dd, 1 H, J_{HH} = 7.0 and 8.1), 7.65 (dd, 1 H, J_{HH} = 7.0 and 8.1), 7.58 (d, 1 H, J_{HH} = 7.8), 7.50 (dd, 1 H, J_{HH} = 7.8 and 7.8), 7.47 (d, 1 H, J_{HH} = 8.4), 7.38 (dd, 1 H, J_{HH} = 7.8 and 7.8), 7.33 (dd, 1 H, J_{HH} = 7.8 and 7.5), 7.15 (d, 1 H, J_{HH} = 9.0), 7.01 (dd, 1 H, J_{HH} = 7.8 and 7.5 Hz), 6.94 (m, 2 H), 4.87 (m, 1 H) and 3.56 (m, 1 H).

X-Ray crystal structure determinations

Single crystals of compounds **1b**, **2**, **4** and **5** for X-ray analyses were obtained as described above. A crystal of cluster **4** was mounted on top of a glass fibre by means of an epoxy resin while complexes **1b**, **2** and **5** were sealed in Lindemann glass capillaries. Crystal intensity data were collected on either a Rigaku-AFC7R or a MAR research image-plate scanner using graphite-monochromated Mo-Kα radiation (λ = 0.710 73 Å) for unit-cell determination and data collection. Summaries of the crystallographic data, structure solution and refinement are given in Table 5. The ω–2θ scan mode with a speed of 16.0° min^{-1} was used for complexes **1b**, **2** and **4**. For cluster **5**, 65 3° frames with an exposure time of 5 min per frame were used. Lorentz, polarisation and ψ scan absorption corrections[18] were applied to all the intensity data collected on a Rigaku-AFC7R diffractometer. However, only Lorentz and polarisation effects were corrected for **5**. Scattering factors were taken from ref. 19(*a*) and anomalous dispersion effects were included in F_c.[19b] The positions of ruthenium atoms were determined by direct methods (SIR 92).[20] The remaining non-hydrogen atoms were determined by subsequent Fourier and Fourier-difference techniques. The structures were refined by full-matrix least-squares analysis on *F* with all non-hydrogen atoms refined anisotropically until convergence was reached. The hydrogen atom of the imido moiety was located by Fourier-difference synthesis while hydrogen atoms of the organic moieties were generated in their ideal positions (C–H, 0.95 Å). They were included in the structure factor calculations but were not refined. All calculations were performed on a Silicon-Graphics computer using the program package TEXSAN.[21]

CCDC reference number 186/626.

Acknowledgements

W.-T. W. acknowledges financial support from the Hong Kong Research Grants Council and the University of Hong Kong. K. K.-H. L. acknowledges the receipt of a postgraduate studentship, administered by the University of Hong Kong.

References

1 W. Bartok, A. R. Crawford and A. Skapp, *Chem. Eng. Prog.*, 1971, **67**, 64; 'Air Pollution', ACS Repr. Collect. Am. Chem. Soc., Washington, D.C., 1973.
2 J. A. Smieja and W. L. Gladfelter, *Inorg. Chem.*, 1986, **25**, 2667; S. Bhaduri, K. S. Gopalkrishnan, G. M. Sheldrick, W. Clegg and D. Stalke, *J. Chem. Soc., Dalton Trans.*, 1983, 2339.
3 S. Bhaduri, K. S. Gopalkrishnan, W. Clegg, P. G. Jones, G. M. Sheldrick and D. Stalke, *J. Chem. Soc., Dalton Trans.*, 1984, 1765.
4 K. K. H. Lee and W. T. Wong, *J. Chem. Soc., Dalton Trans.*, 1996, 3911.
5 B. Foretic, N. Burger and V. Hankonyi, *Polyhedron*, 1995, **14**, 605.

6 O. K. Borggaard, H. E. M. Christensen, T. K. Nielsen and M. Willems, *Analyst* (*London*), 1982, **107**, 1479; O. K. Borggaard, H. E. M. Christensen and S. P. Lund, *Analyst* (*London*), 1984, **109**, 1179; M. I. Gromova and A. N. Gonik, *Zh. Anal. Khim.*, 1984, **39**(2), 307; J. Kurpiewska, *Pr. Cent. Inst. Ochr. Pr.*, 1982, **32**, 107.
7 K. B. Chakroborty, G. Scott and H. Yaghmour, *J. Appl. Polym. Sci.*, 1985, **30**(1), 189; J. Novak, J. Mleziva and J. Eichler, *Angew. Makromol. Chem.*, 1984, **128**, 123.
8 (*a*) R. G. Buckley, J. Charalambous, M. J. Kensett, M. McPartlin, P. Mukerjee, E. G. Brain and J. M. Jenkins, *J. Chem. Soc., Perkin Trans. 1*, 1983, 693; (*b*) J. Charalambous, K. Henrick, Y. Musa, R. G. Rees and R. N. Whiteley, *Polyhedron*, 1987, **6**, 1509; (*c*) H. Saarinen and J. Korvenranta, *Acta Chem. Scand., Ser. A*, 1975, **29**, 409; (*d*) J. Charalambous, W. C. Stoten and K. Henrick, *Polyhedron*, 1989, **8**, 103.
9 H. Alper and J. T. Edward, *Can. J. Chem.*, 1970, **48**, 1543.
10 J. Charalambous, L. I. B. Haines, J. S. Morgan, D. S. Peat, M. J. M. Campbell and J. Bailey, *Polyhedron*, 1987, **6**, 1027.
11 L. A. Hoferkamp, G. Rheinwald, H. Stoeckli-Evans and G. Süss-Fink, *Organometallics*, 1996, **15**, 704.
12 C. K. Johnson, ORTEP, Report ORNL-5138, Oak Ridge National Laboratory, Oak Ridge, TN, 1976.
13 J. A. van Doorn and P. W. N. M. van Leeuwen, *J. Organomet. Chem.*, 1981, **222**, 299.
14 S. Aime, G. Gervasio, L. Milone, R. Rossetti and P. L. Stanghellini, *J. Chem. Soc., Dalton Trans.*, 1978, 534.
15 G. P. Khare and R. J. Doedens, *Inorg. Chem.*, 1976, **15**, 86.
16 R. G. Buckley, J. Charalambous and K. F. Henrick, *Acta Crystallogr., Sect. B*, 1982, **38**, 289.
17 J. Charalambous, R. G. Buckley and E. G. Brain, *J. Chem. Soc., Perkin Trans. 1*, 1982, 1075.
18 A. C. T. North, D. C. Phillips and F. S. Mathews, *Acta Crystallogr., Sect. A*, 1968, **24**, 351.
19 D. T. Cromer and J. T. Waber, *International Tables for X-Ray Crystallography*, Kynoch Press, Birmingham, 1974, vol. 4; (*a*) Table 2.2.B; (*b*) Table 2.3.1.
20 M. C. Burla, M. Camalli, G. Cascarano, C. Giacovazzo, G. Polidori, R. Spagna and D. Viterbo, *J. Appl. Crystallogr.*, 1989, **22**, 389.
21 TEXSAN, Crystal Structure Analysis Package, Molecular Structure Corporation, Houston, TX, 1985 and 1992.

Received 13*th May* 1997; *Paper* 7/03307I